Proc. R. Soc. Lond. A **382**, 411–428 (1982)
Printed in Great Britain

Excitation of surface waves by sub-surface sources

BY J. D. ACHENBACH AND A. NORRIS
The Technological Institute, Northwestern University, Evanston, Illinois 60201, *U.S.A.*

(*Communicated by D. S. Jones, F.R.S. – Received* 14 *December* 1981)

A method is proposed for the determination of surface waves produced by a buried source in a half-space. The analytical problem may be divided into two distinct cases, in which the source region is compact or non-compact. For a compact source the angular variation of the outgoing field may be characterized by an analytic function, which we call the 'emission' function. By the use of a representation integral, the surface wave is related to the value of the emission function at a complex angle. The emission function may be approximated by the full-space emission function or its ray-theory representation. As an example of a compact source, a cylindrical cavity with a concentrated line source on its circumference is considered. It is shown that the cavity may have an amplifying effect on surface-wave excitation. Diffraction by a semi-infinite screen is investigated as an example of surface waves generated by a non-compact source. The emission function for the screen, as well as its ray-theory approximation, are not analytic, and the consequent complications are discussed. The general results of this paper provide a means of analysing the excitation of surface waves by combining the intuitively simple aspects of ray theory in real space with a classical integral representation of the wave field.

INTRODUCTION

A surface wave propagates in a direction tangential to a surface, while its amplitude decays exponentially in the normal direction. The existence of surface waves depends on the boundary condition. For time-harmonic wave motions governed by the scalar wave equation, surface waves are possible for an impedance boundary condition. For a half-space ($y \geqslant 0$), an impedance boundary condition is defined by

$$\partial u/\partial y = -\mathrm{i}kZu, \quad y = 0, -\infty < x, z < \infty, \tag{1.1}$$

where $u(\boldsymbol{x})$ satisfies the reduced wave equation

$$\nabla^2 u + k^2 u = 0, \tag{1.2}$$

k is the wavenumber, and Z the impedance. A condition of the form (1.1) is frequently used in acoustics and electromagnetic theory to approximate the effect of a surface layer.

This paper is concerned with the excitation of time-harmonic surface waves by two-dimensional source mechanisms in the interior of a half-space. For a buried line source parallel to the surface $y = 0$, an expression for the surface wave can be obtained by the use of Fourier-transform methods. Mathematically, the surface wave corresponds to the residue from a pole in the plane of the complex Fourier-transform variable.

For a large class of problems it is not possible to express the field at $y = 0$ in terms of Fourier integrals over known functions. Radiation from an interior cavity of arbitrary shape, either by direct excitation at its surface, or because the cavity acts as a wave scatterer, is an example. For such problems this paper gives an expression for the surface wave as a path-independent integral. The surface of integration, S, is arbitrary to the extent that the sources must be inside S, and the point of observation must be exterior to S. An analytic function, called the 'emission function', is introduced. This function completely defines the angular variation of the outgoing field. The surface-wave amplitude is shown to be equal to the value of the emission function at a complex angle that depends on the impedance Z of (1.1). For the line source this approach reproduces the result of Keller & Karal (1960).

In practice, the emission function for the half-space geometry is generally unobtainable. However, it may be approximated by the corresponding full-space emission function $E(\theta)$. By using this approximation, only the first interaction between source and surface is taken into account. As an example, surface waves generated by the application of a line force along a generator of a buried circular cavity are investigated. The exact full-space emission function $E(\theta)$ is derived and shown to be analytic. Numerical results for the surface waves are presented. The effect of creeping waves on the generated surface-wave motion is noticeable for certain combinations of the impedance, the angle defining the position of the applied force and the dimensionless number ka (the product of wavenumber and cavity radius). For other combinations of these parameters, it is shown that a simple 'ray-theory' form of $E(\theta)$ gives results that compare well with those corresponding to the exact emission function. A comparison of the amplitudes of surface waves generated by a line load on the surface of a cavity and by a point load at the same location in an homogeneous half-plane shows that the presence of the cavity may have an amplifying effect.

It is clearly convenient to investigate first the waves radiated from a source region as if the medium were unbounded, and then to proceed with an examination of the interaction of these waves with the surface of the half-space. As an alternative to the use of the integral representation, a formal description of this approach can be given with the aid of geometrical ray theory. The disturbances generated at the surface of the cavity propagate along straight rays. Far away (or at high frequencies) the ray fields can be expressed simply. When rays intersect a boundary at which (1.1) holds, reflected rays and rays of surface-wave motion are generated. The fields on reflected rays can easily be analysed. To investigate rays of surface-wave motion, Keller & Karal (1960) considered the two-dimensional canonical problem of a line source. They showed that surface-wave motions require the introduction of rays in complex space. For more complicated sources, the same formalism of complex rays can be used. In §4, we consider the two-dimensional canonical problem of an arbitrary source. The results of that section may be viewed as a justification of the extension of complex ray theory to include arbitrary sources.

The general results of this provide a means to combine the intuitively simple aspects of ray theory in real space with a classical integral representation of the wave field. In particular, for more complicated geometries the approach of the present paper removes the necessity of tracing complex rays whose geometrical properties are ambiguous.

In a second example, surface waves induced by the presence of a non-compact scatterer are investigated. The scatterer is a semi-infinite screen below the impedance surface. An incident surface wave interacts with the screen and generates a diffracted field radiating from the screen's edge. The diffracted field induces forward- and back-scattered surface waves. Although the emission function is not analytic, the method of this paper is applied. Some deficiencies occur at certain orientations of the screen. The results apply to diffraction of Love waves by the tip of a sub-surface crack.

2. Wave motion in the half-plane

First, let us consider surface waves when there are no sources present, and (1.2) is satisfied in the whole half-plane $-\infty < x < \infty$, $y \geqslant 0$. The boundary condition at $y = 0$ is given by (1.1). There are two essentially different elementary solutions. The first is the system of incident and reflected plane waves represented by

$$u^{\mathrm{p}} = \mathrm{e}^{\mathrm{i}kx\cos\alpha}[\mathrm{e}^{-\mathrm{i}ky\sin\alpha} + R(\alpha)\,\mathrm{e}^{\mathrm{i}ky\sin\alpha}], \tag{2.1}$$

where α is the angle of incidence depicted in figure 1, and $R(\alpha)$ is the reflexion coefficient

$$R(\alpha) = (\sin\alpha - Z)/(\sin\alpha + Z). \tag{2.2}$$

The second non-trivial solution is the surface wave, defined by

$$u^{\mathrm{s}}(\pm x, y) = \tan\phi \exp\left[\mathrm{i}k(\pm x\cos\phi + y\sin\phi)\right], \tag{2.3}$$

where the sign $(\pm)$ indicates the direction of propagation along the x-axis, and

$$\phi = \arcsin(-Z). \tag{2.4}$$

We include the factor $\tan\phi$ in the definition of u^{s} to simplify expressions later. From (2.4) it is evident that u^{s} remains bounded only if Z is negative imaginary. If this is so, let Y be a positive real number. Then

$$Z = -\mathrm{i}Y, \tag{2.5}$$

in which case by (2.4)

$$\phi = \mathrm{i}\,\mathrm{arsinh}\, Y. \tag{2.6}$$

Next we consider forced wave motion generated by a point source at (x_0, y_0). The solution is the Green function u^{G}, where

$$\nabla^2 u^{\mathrm{G}} + k^2 u^{\mathrm{G}} = -\delta(x - x_0)\,\delta(y - y_0), \tag{2.7}$$

governs u^{G} in the half-plane $y \geqslant 0$, while the boundary condition at $y = 0$ is given by (1.1). The solution has been given by Keller & Karal (1960) as

$$u^{\mathrm{G}} = u^{\mathrm{f}} + u^{\mathrm{r}}. \tag{2.8}$$

Here u^{f} is the full-space solution defined by

$$u^{\mathrm{f}} = \tfrac{1}{4}\mathrm{i}H_0^{(1)}(kr) \tag{2.9}$$

where

$$r = [(x-x_0)^2 + (y-y_0)^2]^{\frac{1}{2}}, \tag{2.10}$$

and u^{r} is the 'reflected' wave,

$$u^{\mathrm{r}} = \frac{\mathrm{i}}{4\pi}\int_{\mathscr{C}} R(\alpha)\exp\{\mathrm{i}k[|x-x_0|\cos\alpha + (y+y_0)\sin\alpha]\}\,\mathrm{d}\alpha. \tag{2.11}$$

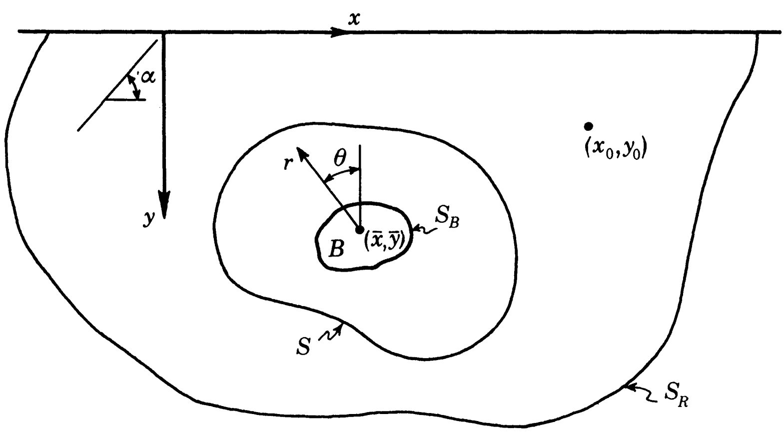

FIGURE 1. Source region B in the half-plane $y > 0$, and surfaces of integration.

In (2.11), the contour $\mathscr{C}$ is the Sommerfeld contour in the complex α-plane. There is a pole at $\alpha = \phi$, where ϕ is defined in (2.4). In deforming to the steepest-descent contour, we pick up a contribution from the pole only when

$$(y+y_0)/|x-x_0| < \tan\{\mathrm{Re}\,(\phi) + \arcsin\,[\tanh\,(\mathrm{Im}\,\phi)]\}. \tag{2.12}$$

The pole contribution is a surface wave denoted by $u^{\mathrm{G,s}}$,

$$\begin{aligned} u^{\mathrm{G,s}} &= \tan\phi\exp\{\mathrm{i}k[|x-x_0|\cos\phi + (y+y_0)\sin\phi]\} \\ &= u^{\mathrm{s}}(|x-x_0|, y+y_0), \end{aligned} \tag{2.13}$$

where $u^{\mathrm{s}}(\,,\,)$ is defined by (2.3). For $u^{\mathrm{G,s}}$ to remain bounded, we must have

$$\mathrm{Re}\,Z \geqslant 0, \quad \mathrm{Im}\,Z < 0. \tag{2.14}$$

For a point source, we may have surface-type waves that decay in the x-direction as well as in the y-direction. These are referred to as 'leaky' waves. When $\mathrm{Re}\,Z = 0$, we get true surface waves which may propagate indefinitely in the x-direction. In this case, we have as before that $Z = -\mathrm{i}Y$, and the inequality (2.12) reduces to

$$(y+y_0)/|x-x_0| < Y. \tag{2.15}$$

In addition to the pole contribution to u^{G} by (2.11), there are contributions from the steepest-descent integral. The latter effects may be shown to be $O[(kr)^{-\frac{1}{2}}]$, away from the source. Also, we see directly that u^{f} of (2.9) is $O[(kr)^{-\frac{1}{2}}]$. Thus

$$u^{\mathrm{G}} = u^{\mathrm{G,s}} + O[(kr)^{-\frac{1}{2}}]. \tag{2.16}$$

Now, as $|x| \to \infty$, we have that

$$u^{\mathrm{G,s}} = O(\exp[-k\,|x-x_0|\,\mathrm{Im}\,(\cos\phi)]). \tag{2.17}$$

Therefore u^{G} may be approximated asymptotically by $u^{\mathrm{G,s}}$ only if $Z = -\mathrm{i}Y$. In other words, leaky waves are confined to the region of the epicentre $(x_0, 0)$, where they are indistinguishable from the body waves emitted by the sources.

3. Path-independent integrals

Consider a region of volume V bounded by a closed surface S. From the divergence theorem it follows that two scalar functions $u(\boldsymbol{x})$ and $v(\boldsymbol{x})$ satisfy the Green second identity

$$\mathscr{L}(u, v; S) = \int_V (u\,\nabla^2 v - v\,\nabla^2 u)\,\mathrm{d}V, \tag{3.1}$$

where the operator $\mathscr{L}(u, v; S)$ is defined as

$$\mathscr{L}(u, v; S) = \int_S (u\,\nabla v - v\,\nabla u)\cdot\boldsymbol{n}\,\mathrm{d}S. \tag{3.2}$$

The functions u and v, and their first- and second-order derivatives are continuous, and $\boldsymbol{n}$ is the unit outward normal to S.

In the interior of a half-space we now consider a region B that emits wave motions. The region B may contain volume sources, or it may be a cavity whose surface S_B is subjected to excitations. The region outside the source region B is denoted V_B. The geometry is shown in figure 1. The wave field generated by B, $u_B(\boldsymbol{x})$, satisfies the boundary condition (1.1) at $y = 0$, the reduced wave equation (1.2) in V_B, and appropriate conditions inside B or on the boundary S_B.

Now let us select closed surfaces S and S_R such that B is interior to the space bounded by S, and S is interior to the space bounded by S_R (see figure 1). For v we choose the Green function, $u^{\mathrm{G}}(\boldsymbol{x})$, for the half-space. For the two-dimensional case this function was discussed in § 2, (2.7)–(2.11). Application of (3.2) to u_B and u^{G} in the region bounded by S and S_R yields

$$u_B(\boldsymbol{x}_0) = \mathscr{L}(u_B, u^{\mathrm{G}}; S) - \mathscr{L}(u_B, u^{\mathrm{G}}; S_R). \tag{3.3}$$

By virtue of the Sommerfeld radiation condition the integral over S_R vanishes as $R \to \infty$. Hence

$$u_B(\boldsymbol{x}_0) = \mathscr{L}(u_B, u^{\mathrm{G}}; S). \tag{3.4}$$

Clearly the integral in (3.4) is path-independent, since S is arbitrary, as long as B is located in the space interior to S and $\boldsymbol{x}_0$ is located outside S.

Let us now examine the nature of u_B. We define as $u_{B,0}$ the field produced if the same source region were situated in a homogeneous full space. The difference between u_B and $u_{B,0}$ comes from the multiple reflexion and scattering between the surface of the half-space and B. The primary wave $u_{B,0}$ interacts with the surface $y = 0$, producing reflected waves; and surface waves; these reflected waves interact with B, producing scattered outgoing waves from B, and so on. Thus, in addition to $u_{B,0}$, the radiated field u_B is equal to an infinite sum of reflected waves and surface waves, defined as $u_{B,\mathrm{re}}$, plus an infinite sum of scattered outgoing waves from B, defined as $u_{B,\mathrm{sc}}$. We may write

$$u_B = u_{B,0} + u_{B,\mathrm{sc}} + u_{B,\mathrm{re}}. \tag{3.5}$$

In general it is possible to define $u_{B,\mathrm{re}}$ and $u_{B,\mathrm{sc}}$ uniquely. For example, suppose B is a void with surface S_B, subjected to prescribed values $u_B = \bar{u}_{B,0}$. Let us consider the following problem for the half-space $y \geqslant 0$:

$$\nabla^2 u + k^2 u = 0, \quad -\infty < x, z < \infty, \quad y > 0, \tag{3.6a}$$

$$\partial u/\partial y + \mathrm{i}kZu = f, \quad -\infty < x, z < \infty, \quad y = 0. \tag{3.6b}$$

In operator form the solution is denoted by

$$u = M(f). \tag{3.7}$$

We also consider a problem for the *full* space outside the region B:

$$\nabla^2 v + k^2 v = 0, \quad \boldsymbol{x} \in \mathscr{R}^3/B, \tag{3.8a}$$

$$v = \bar{v}, \quad \boldsymbol{x} \in S_B. \tag{3.8b}$$

The operator form of the solution is denoted by

$$v = N(\bar{v}). \tag{3.9}$$

Both solutions u and v also satisfy radiation conditions. Let us now define

$$u_1 = M\{-[\partial u_{B,0}/\partial y + \mathrm{i}kZu_{B,0}]_{y=0}\}, \tag{3.10}$$

$$v_j = N(-\bar{u}_j), \quad j \geqslant 1, \tag{3.11}$$

$$u_{j+1} = M\{-[\partial v_j/\partial y + \mathrm{i}kZv_j]_{y=0}\}, \quad j \geqslant 1. \tag{3.12}$$

Then

$$u_{B,\mathrm{re}} = \sum_{j=1}^{\infty} u_j; \quad u_{B,\mathrm{sc}} = \sum_{j=1}^{\infty} v_j. \tag{3.13a, b}$$

This iterative procedure has been used by Thiruvenkatachar & Viswanathan (1965) in considering the response of an elastic half-space to a loaded spherical cavity in its interior.

Substitution of the representation (3.4) into (3.5) yields $u_B(\boldsymbol{x}_0)$ as

$$u_B(\boldsymbol{x}_0) = \mathscr{L}(u_{B,0}, u^{\mathrm{G}}; S) + \mathscr{L}(u_{B,\mathrm{sc}}, u^{\mathrm{G}}; S) + \mathscr{L}(u_{B,\mathrm{re}}, u^{\mathrm{G}}; S). \tag{3.14}$$

The term $\mathscr{L}(u_{B,\mathrm{re}}, u^{\mathrm{G}}; S)$ can be converted into a volume integral over the region interior to S by the use of (3.1). Since both $u_{B,\mathrm{re}}$ and u^{G} satisfy a homogeneous wave equation inside S, this term vanishes, and thus

$$u_B(\boldsymbol{x}_0) = \mathscr{L}(u_{B,0} + u_{B,\mathrm{sc}}, u^{\mathrm{G}}; S). \tag{3.15}$$

4. Excitation of surface waves by compact sources

In the remainder of this paper we consider a two-dimensional geometry. Let us take a new origin at some point $P(\bar{x}, \bar{y})$ which is in or near B. With respect to this origin we define a polar coordinate system, (r, θ), $0 \leqslant r < \infty$, $-\pi \leqslant \theta \leqslant \pi$, as shown in figure 1, i.e.

$$x-\bar{x} = -r\sin\theta, \quad y-\bar{y} = -r\cos\theta. \tag{4.1}$$

Consider the outgoing field $u_{B,0}$. This field is regular outside some surface S_B that encloses B and P. It is known that any such field may be expressed as

$$u_{B,0} = (\tfrac{1}{2}\pi)^{\frac{1}{2}} e^{\frac{1}{4}i\pi} \sum_{n=-\infty}^{\infty} E_n H_n^{(1)}(kr)\, e^{in(\theta+\frac{1}{2}\pi)}, \tag{4.2}$$

for some set $\{E_n\}$. In other words, the eigenfunctions $\{H_n^{(1)}(kr)\, e^{in\theta}\}$ are complete for the solutions of $(\nabla^2+k^2)\, u = 0$ in $\mathscr{R}^2/S_B$ that are outgoing.

Let d be the maximum distance from P to the surface S_B. We use the asymptotic result for Hankel functions of large order,

$$H_n^{(1)}(\lambda) \sim -\left(\frac{2}{\pi\,|n|}\right)^{\frac{1}{2}} \left(\frac{2n}{e\lambda}\right)^{|n|}. \tag{4.3}$$

At the point on S_B a distance d from P, the field as given by (4.2) must be bounded. Therefore, by (4.3) we require that, for $|n|$ large and $|n| \gg kd$,

$$E_n = o[|n|^{\frac{1}{2}}\,(2n/ekd)^{-|n|}]. \tag{4.4}$$

Let us now define the far-field emission function $E(\theta)$ as

$$E(\theta) = \lim_{r\to\infty} [(kr)^{\frac{1}{2}}\, e^{-ikr} u_{B,0}]. \tag{4.5}$$

From (4.2) and the result that, as $|\lambda| \to \infty$,

$$H_n^{(1)}(\lambda) = (2/\pi\lambda)^{\frac{1}{2}}\, e^{i(\lambda-\frac{1}{2}n\pi-\frac{1}{4}\pi)}[1+O(1/\lambda)], \tag{4.6}$$

we get

$$E(\theta) = \sum_{n=-\infty}^{\infty} E_n\, e^{in\theta}. \tag{4.7}$$

Thus the constants E_n are the Fourier coefficients of $E(\theta)$:

$$E_n = (2\pi)^{-1}\int_0^{2\pi} E(\theta)\, e^{-in\theta}\, d\theta. \tag{4.8}$$

It follows from (4.4) that $E(\theta)$ is analytic for any finite complex θ.

Equations (4.2) and (4.8) show that $E(\theta)$ defines $u_{B,0}$ in $\mathscr{R}^2/S_B$. Similarly, with respect to the same origin, the field $u_{B,\mathrm{sc}}$ is uniquely determined by an analytic function $E_{\mathrm{sc}}(\theta)$ or its Fourier coefficients.

Now we return to the integral expression (3.15). Suppose we wish to investigate the surface motion at $(x_0, 0)$ produced by excitation in B. The point source will then be located at $(x_0, 0)$. For the boundary condition given by $Z = -iY$, i.e. in the absence of leaky waves, the dominant part of u^{G} sufficiently far from $(x_0, 0)$ is given by $u^{G,s}$. We define $u_B^s(x_0, 0)$ as

$$u_B^s(x_0, 0) = \mathscr{L}(u_{B,0} + u_{B,\mathrm{sc}}, u^{G,s}; S). \tag{4.9}$$

The surface S is arbitrary, provided that S surrounds B and $(x_0, 0)$ is outside S. To express the surface wave $u^{G,s}$ at $(x_0, 0)$ due to a point source at (x, y) in the polar coordinate system (4.1), we assume first that for all points in B

$$x_0 - x \gg \bar{y}. \tag{4.10}$$

Then (2.13) can be written

$$u^{G,s} = U^s \exp[\mathrm{i}kr \sin(\theta - \phi)], \tag{4.11}$$

where

$$U^s = \tan\phi \exp\{\mathrm{i}k[(x_0 - \bar{x})\cos\phi + \bar{y}\sin\phi]\}. \tag{4.12}$$

Let

$$u_n \equiv H_n^{(1)}(kr)\, \mathrm{e}^{\mathrm{i}n\theta}. \tag{4.13}$$

Then

$$\mathscr{L}(u_n, u^{G,s}; S) = U^s kr \int_0^{2\pi} \{\mathrm{i}H_n^{(1)}(kr)\sin(\theta-\phi) - [H_n^{(1)}(kr)]'\} \times \exp \mathrm{i}[kr\sin(\theta-\phi) + n\theta]\,\mathrm{d}\theta, \tag{4.14}$$

where the prime denotes differentiation with respect to the argument. Explicit integration yields Bessel functions of the first kind. Further simplification is obtained by using the result for the Wronskian of Bessel functions:

$$J_\nu(z)\, Y_\nu'(z) - J_\nu'(z)\, Y_\nu(z) = 2/\pi z. \tag{4.15}$$

The final result is

$$\mathscr{L}(u_n, u^{G,s}; S) = 4U^s\, \mathrm{e}^{\mathrm{i}[n(\phi-\pi) - \frac{1}{2}\pi]}. \tag{4.16}$$

Substitution of $u_{B,0}$ as given by (4.2), together with the corresponding expression for $u_{B,\mathrm{sc}}$ in (4.9), yields upon the use of (4.16)

$$u_B^s(x_0, 0) = (8\pi)^{\frac{1}{2}}\, \mathrm{e}^{-\frac{1}{4}\mathrm{i}\pi}[E(\phi - \tfrac{1}{2}\pi) + E_{\mathrm{sc}}(\phi - \tfrac{1}{2}\pi)]\, U^s. \tag{4.17}$$

This result is exact to the extent that only the surface-wave part of the Green function has been used. Thus the expression in (4.17) does not take into account the effect of body waves on the surface displacement, but this effect is asymptotically negligible in the far field. From (4.10) it is evident that (4.17) corresponds to the forward-scattered surface wave, i.e. the wave propagating in the positive x-direction. The back-scattered surface wave may be considered similarly. We find, for $x_0 > 0$, that

$$u_B^s(\pm x_0, 0) = (8\pi)^{\frac{1}{2}}\, \mathrm{e}^{-\frac{1}{4}\mathrm{i}\pi}[E(\pm(\phi - \tfrac{1}{2}\pi)) + E_{\mathrm{sc}}(\pm(\phi - \tfrac{1}{2}\pi))]\, U^s(\pm x_0). \tag{4.18}$$

We now apply this result to two examples of two-dimensional compact sources. The first example is the trivial case of an isotropic point source.

Two-dimensional point source

The outgoing field for a point source at $(\bar{x}, \bar{y})$ is given by (2.9). By (4.5) and (4.6) we have

$$E(\theta) = (8\pi)^{-\frac{1}{2}}\, \mathrm{e}^{\frac{1}{4}\mathrm{i}\pi}. \tag{4.19}$$

Since the source is a point source, the multiply scattered field $u_{B,\,\mathrm{sc}}$ is zero. Hence $E_{\mathrm{sc}} = 0$ and from (4.17) we derive the expected identity

$$u_B^{\mathrm{s}}(x_0, y_0) = u^{\mathrm{G,s}}(\bar{x}, \bar{y}), \tag{4.20}$$

where $u^{\mathrm{G,s}}$ is given by (2.13). Thus (4.17) predicts the correct surface wave due to a point source.

Line force on a circular cylindrical cavity

Next, we consider a two-dimensional problem for a half-space containing a circular cylindrical cavity with the cavity axis parallel to the surface. A line force parallel to the axis is located on the circumference of the cylinder. The two-dimensional geometry is depicted in figure 2.

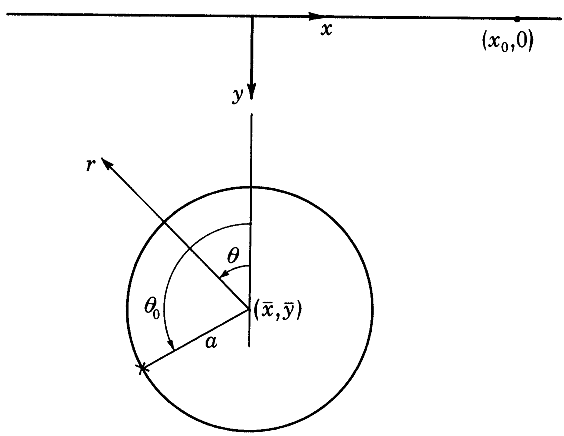

FIGURE 2. Buried cylindrical cavity with a line force on its circumference.

The emission function $E(\theta)$ for the full-space problem can be determined explicitly. The multiply scattered emission function E_{sc} will be non-zero, but we assume that it can be neglected. Thus we are concerned only with the first mutual interaction between source and surface. From the view of superposition of harmonics to obtain a pulse in the time domain, this approximation implies that attention is restricted to the surface waves arriving first. An alternative interpretation follows from the work of Gregory (1970). He considered the response of an elastic half-space with a cylindrical cavity present. For arbitrary loading on the cavity, he derived a low frequency ($ka \to 0$) asymptotic representation for the field. A similar analysis for the present scalar problem shows that our surface-wave approximation is the first term in a low frequency asymptotic series.

With respect to a polar coordinate system whose origin is at the centre of the cavity of radius a, the boundary condition on the cavity surface is

$$\partial u/\partial r = k\,\delta(\theta - \theta_0), \quad r = a. \tag{4.21}$$

Here $\delta(\;)$ is the Dirac δ-function and $\theta_0 \in [0, 2\pi)$ defines the position on the circumference at which the point force is applied (see figure 2). Since we are interested in the emission function $E(\theta)$ for the full-space problem, we may take $\theta_0 = 0$ for convenience of notation. At a later stage we shall give numerical examples for the full range of θ_0. For the boundary condition (4.21), the solution of the reduced wave equation (1.2) with an appropriate radiation condition in the exterior of the circle is

$$u = (2\pi)^{-1} \sum_{n=-\infty}^{\infty} \frac{H_n^{(1)}(kr)}{[H_n^{(1)}(ka)]'} e^{in\theta}, \tag{4.22}$$

where, as earlier, the prime denotes differentiation with respect to the argument. The emission function $E(\theta)$ follows by use of (4.5) and (4.6) as

$$E(\theta) = 2(2\pi)^{-\frac{3}{2}} e^{-\frac{1}{4}i\pi} \sum_{n=0}^{\infty} \epsilon_n \frac{e^{-\frac{1}{2}in\pi}}{[H_n^{(1)}(ka)]'} \cos n\theta, \tag{4.23}$$

where
$$\epsilon_0 = 1, \quad \epsilon_n = 2, \quad n > 0. \tag{4.24}$$

An alternative form for $E(\theta)$ can be deduced by applying the Poisson summation formula to (4.23) (see for example Morse & Feshbach 1953). The result is

$$E(\theta) = 2(2\pi)^{-\frac{3}{2}} e^{-\frac{1}{4}i\pi} \sum_{n=-\infty}^{\infty} \int_{-\infty}^{\infty} \frac{e^{i\nu(\theta-\frac{1}{2}\pi-2n\pi)}}{[H_\nu^{(1)}(ka)]'} d\nu. \tag{4.25}$$

The integration may be performed by changing the contour of integration to enclose the roots $\pm\nu_s$, $s = 1, 2, \ldots$, of $[H_\nu^{(1)}(ka)]' = 0$. The roots ν_s all lie in the first quadrant. Therefore the summation over n can also be performed (see for example Jones 1979). We obtain

$$E(\theta) = \sum_{s=1}^{\infty} E_s(\theta), \tag{4.26}$$

where
$$E_s(\theta) = \frac{(2/\pi)^{\frac{1}{2}} e^{\frac{1}{4}i\pi} [e^{i\nu_s(\theta-\frac{1}{2}\pi)} + e^{i\nu_s(\frac{3}{2}\pi-\theta)}]}{[\tilde{H}_{\nu_s}^{(1)}(ka)]' (1 - e^{i\nu_s 2\pi})}, \tag{4.27}$$

and
$$[\tilde{H}_{\nu_s}^{(1)}(ka)]' \equiv \partial[H_\nu^{(1)}(ka)]'/\partial\nu|_{\nu=\nu_s}. \tag{4.28}$$

It should be noted that $\operatorname{Re}\theta \in [0, 2\pi)$ is understood in (4.27).

For real θ and $ka \gg 1$, the emission function possesses an aymptotic approximation, valid for θ not near $\frac{1}{2}\pi$ or $\frac{3}{2}\pi$. In the region $\theta \in (\frac{1}{2}\pi, \frac{3}{2}\pi)$, it is seen that the $E_s(\theta)$ of (4.27) are rapidly convergent functions. The terms E_s are often referred to as 'creeping waves', and the region $\theta \in (\frac{1}{2}\pi, \frac{3}{2}\pi)$ is known as the 'shadow region'. In the high frequency range, $ka \gg 1$, the roots ν_s, $s = 1, 2, \ldots$, are approximately (see Jones 1979)

$$\nu_s \sim ka - (\tfrac{1}{2}ka)^{\frac{1}{3}} e^{\frac{1}{3}i\pi} \alpha_s, \tag{4.29}$$

where α_s are the roots of
$$[\operatorname{Ai}(\alpha)]' = 0, \tag{4.30}$$

and Ai( ) is the Airy function. These roots are all real and negative. So, when $\theta \in (\frac{1}{2}\pi, \frac{3}{2}\pi)$ we may approximate $E(\theta)$ by the first term of the creeping-wave expansion. Also, we can use the approximation

$$[\tilde{H}_{\nu_s}^{(1)}(ka)]' \sim 4\alpha_s \operatorname{Ai}(\alpha_s)/ka \tag{4.31}$$

to simplify the expression for $E_1(\theta)$. Thus, in the shadow region,

$$\begin{aligned} E(\theta) &\sim E_1(\theta) \\ &\sim ka(8\pi)^{-\frac{1}{2}}\,e^{\frac{1}{4}i\pi}[e^{i\nu_1(\theta-\frac{1}{2}\pi)}+e^{i\nu_1(\frac{3}{2}\pi-\theta)}]/\alpha_1\,\mathrm{Ai}\,(\alpha_1) \end{aligned} \tag{4.32}$$

where $\alpha_1 = -1.0188, \quad \mathrm{Ai}\,(\alpha_1) = 0.5357,$

and ν_1 follows from (4.29).

The high frequency approximation to $E(\theta)$ on the 'illuminated' side $\theta \notin [\frac{1}{2}\pi, \frac{3}{2}\pi]$, follows from (4.25). For $|x-\nu| \gg x^{\frac{1}{3}}$, we have that

$$[H_\nu^{(1)}(x)]' \sim x^{-1}(2/\pi)^{\frac{1}{2}}\,(x^2-\nu^2)^{\frac{1}{4}}\,e^{i[\frac{1}{4}\pi+(x^2-\nu^2)^{\frac{1}{2}}-\nu\,\mathrm{arcsec}\,(x/\nu)]}. \tag{4.33}$$

Substitution of this approximation in (4.25) gives

$$\begin{aligned} E(\theta) \sim ka\pi^{-1}\,e^{-\frac{1}{2}i\pi} \sum_{n=-\infty}^{\infty} \int_0 [(ka)^2-\nu^2]^{-\frac{1}{4}} \cos\,[\nu(\theta-2n\pi)] \\ \times e^{-i\nu\{\frac{1}{2}\pi+[(ka/\nu)^2-1]^{\frac{1}{2}}-\mathrm{arcsec}\,(ka/\nu)\}}\,d\nu. \end{aligned} \tag{4.34}$$

The lack of an upper limit on the integral indicates that we assume the dominant contribution to the integral occurs for ν such that the approximation (4.33) is valid. A point of stationary phase occurs only if $\theta \notin [\frac{1}{2}\pi, \frac{3}{2}\pi]$, i.e. the point of observation is on the 'illuminated' side. The stationary-phase point is at

$$\nu = ka\,|\sin\theta|. \tag{4.35}$$

The steepest-descents approximation yields

$$E(\theta) \sim ka(2\pi)^{-\frac{1}{2}}\,e^{-i(\frac{3}{4}\pi+ka\cos\theta)} \equiv E_{\mathrm{rt}}. \tag{4.36}$$

Equations (4.32) and (4.36) give us two distinct approximations to $E(\theta)$. We refer to (4.32) as the 'creeping-wave' approximation, and to (4.36) as the 'ray-theory' approximation. We reiterate that they are only valid for θ real and not near the angles $\frac{1}{2}\pi$ or $\frac{3}{2}\pi$.

Now let us return to the problem of evaluating the surface wave produced by the point force on the buried cavity. Neglecting the multiply scattered emission function E_{sc}, we have by (4.17) that the magnitude of the surface wave at the point $(x_0, 0)$ on the surface is

$$u_B^{\mathrm{s}} \equiv (8\pi)^{\frac{1}{2}}\,e^{-\frac{1}{4}i\pi}E(\tfrac{3}{2}\pi-\theta_0+\phi)\,U^{\mathrm{s}}. \tag{4.37}$$

Thus u_B^{s} is equal to the amplitude of the forward-scattered surface wave. In (4.37) U^{s} is the amplitude of the surface wave produced by a point force at the centre of the cavity, if the cavity were not present. The emission function $E(\theta)$ is given in two forms in (4.23) and (4.26). In the following numerical examples we have used the expression of (4.23) since it does not require the computation of the roots of the Hankel functions, which depend on ka. The angle ϕ is taken as that for a pure surface wave. Thus it is imaginary and given by equation (2.6) as a function of the impedance magnitude Y.

Rather than calculate the magnitude of u_B^s in (4.37), which depends on the depth of the cavity below the surface, we have computed the function $\bar{E}$ defined by

$$\bar{E} = |E(\tfrac{3}{2}\pi - \theta_0 + \phi)|. \tag{4.38}$$

The function $\bar{E}$ depends on the impedance Y, the product ka, and the angle θ_0 at which the point force is applied. In figure 3 we have plotted $\lg \bar{E}$ as a function of θ_0 for $ka = 5$ and $Y = 0, 0.5, 1$ and 2. For $Y = 0$ we have $\phi = 0$ and there are no surface waves. However $\bar{E}(Y = 0)$ has physical meaning for the full-space problem. It is

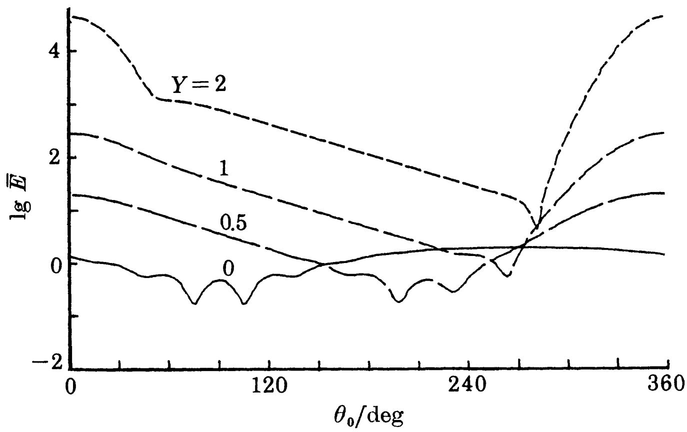

FIGURE 3. Surface-wave amplitude factor $\bar{E}$ plotted against the angle of application, θ_0, of the line force; $ka = 5$.

related by (4.5) to the far field in the direction $\theta = \frac{3}{2}\pi$. We note that it possesses a local maximum at $\theta_0 = \frac{1}{2}\pi$. For $Y > 0$, we observe two distinct types of behaviour from figure 3. Consider for example the curve for $Y = 2$. As θ_0 increases from 0 to *ca.* 60°, $\bar{E}$ decreases approximately as $\exp[-kaY(1-\cos\theta_0)]$. This suggests that the interaction between the point force and the surface is 'direct', since the magnitude decreases in the same manner as for a point source in the absence of the cavity. As θ_0 goes from *ca.* 60° to *ca.* 270°, $\bar{E}$ suffers a linear logarithmic decay, suggesting the presence of creeping-wave effects. Measurements of the amplitude and slopes in figure 3 tally very well with the clockwise creeping wave in (4.32). Similar measurements for other values of ka suggest the interpretation that in this creeping-wave region the surface wave is generated by a creeping wave traversing the cavity circumference in the clockwise direction until it reaches a certain point, dependent on Y and ka, where the interaction is 'direct'. When θ_0 is greater than about 280° (for $Y = 2$) the interaction is again seen to be direct.

In figure 4 we have compared the exact value of $\bar{E}$ with a ray-theory approximation, formed by using the approximate form of $E(\theta)$ given by (4.36) in the equation defining $\bar{E}$, (4.38). In figure 4 the point force is located at the angle θ_0 while the direction of observation is fixed at the (complex) angle $\frac{3}{2}\pi + \phi$. The expression given by (4.36), where the point force is fixed at $\theta = 0$ and the observation direction is arbitrary, was adjusted accordingly for plotting in figure 4. The analysis for (4.36) is only strictly valid for real $\theta \notin [\frac{1}{2}\pi, \frac{3}{2}\pi]$. However, for complex angles it appears from figure 4 to approximate the exact $E(\theta)$ in the 'direct' regions. A similar comparison with the use of the creeping-wave solution of (4.32) gives good agreement in the range of θ_0 where creeping waves are important.

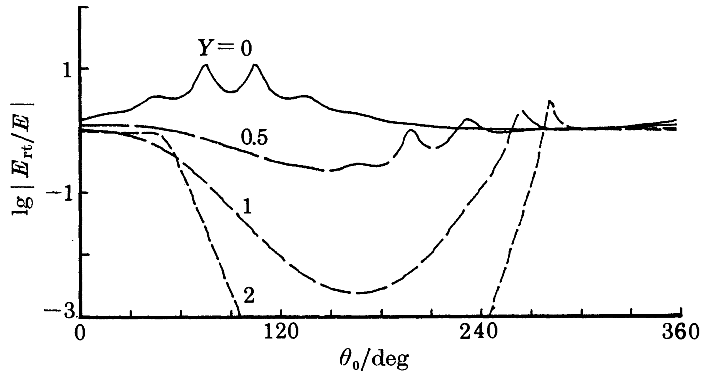

FIGURE 4. Comparison of the ray-theory amplitude, E_{rt}, from (4.36), with the exact result; $ka = 5$.

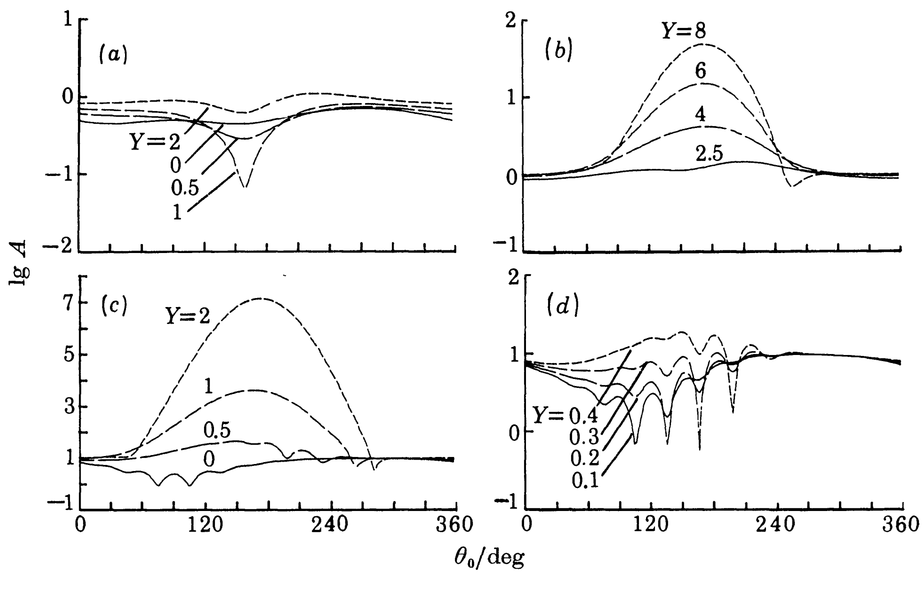

FIGURE 5. Relative amplitude of the surface wave produced by the line force on the cavity and that produced by a line force in the absence of the cavity; (a) (b) $ka = 0.5$; (c), (d) $ka = 5$.

Consider the point force at some angle θ_0 on the cavity (see figure 2). Now suppose we remove the cavity and replace the point force by a point source as in (2.7). We define the cavity amplification factor $A = A(\theta_0, Y, ka)$ as the ratio of the amplitudes of the surface wave produced with the cavity present and when the cavity is removed. In figure 5 we have plotted $\lg A$ for the same values of ka and Y as in figures 3 and 4. We observe that the amplification is almost constant in the 'direct' regions, but that it is very large when the creeping waves are influential. We note that in general the amplification increases as Y increases.

5. Scattering of a surface wave by a semi-infinite sub-surface screen

The theory is now applied to the following problem: a semi-infinite screen is present in the half-space as shown in figure 6. The tip of the screen is at a depth $\bar{y}$. A surface wave is incident from $x = -\infty$. We wish to determine the surface waves on the surface $y = 0$ induced by the presence of the screen.

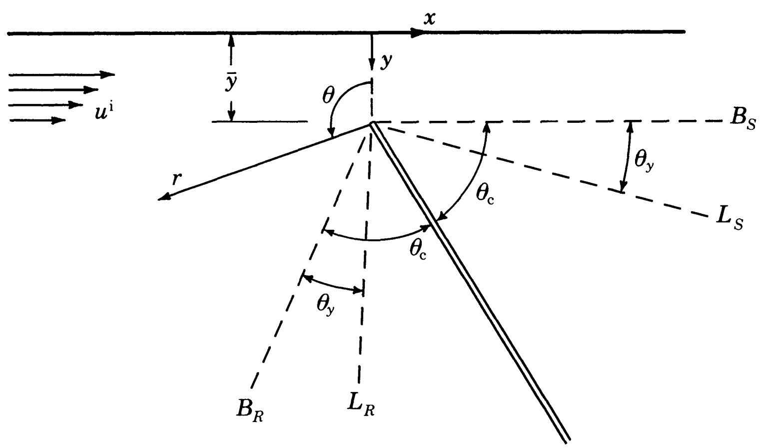

Figure 6. Geometry of semi-infinite sub-surface screen.

In contrast to the examples of the previous section, the scatterer is now non-compact. The analysis leading up to (4.17) is not valid since the surfaces of integration encountered in § 3 cannot be made to enclose the screen. It is not difficult to show that instead of (4.9) we may write

$$u_B^{\mathrm{s}}(x_0, 0) = -\int_0^\infty \frac{1}{r}[u_B(r, \theta_0 + 0^+) - u_B(r, \theta_0 + 0^-)]\, \partial u^{\mathrm{G,s}}(r, \theta_0)/\partial\theta \,\mathrm{d}r, \tag{5.1}$$

where $\theta_0 = \frac{3}{2}\pi - \theta_c$ is the angle defining the screen (see figure 6). We shall consider only the first mutual interaction between the slit and the surface. Then, u_B in (5.1) is replaced by $u_{B,0}$, the outgoing field for the corresponding full-space problem. The expression for the discontinuity of $u_{B,0}$ across the slit, which occurs in the integrand of (5.1), can be deduced from the solution for the classical Sommerfeld diffraction problem. Also, the Green function appearing in (5.1) may be replaced by the expression in (4.11). The integral in (5.1) can be performed explicitly, and the resulting surface-wave amplitude agrees formally with the expression in (4.17); the emission function $E(\theta)$ in (4.17) is discussed below. It turns out that the emission function is not analytic, possessing a simple pole off the real axis. This contrasts with the result of § 4 that the emission function is analytic for compact scatterers.

To determine the emission function $E(\theta)$, we use the results of Deschamps *et al.* (1979) concerning the diffraction of an evanescent plane wave by a semi-infinite screen. Evanescent plane waves are a generalization of homogeneous plane waves to include waves with complex propagation vectors. Deschamps *et al.* discuss the analytic continuation of the Sommerfeld solution for homogeneous plane waves incident upon a semi-infinite screen. Their results are summarized here for convenience.

Let the incident surface wave be

$$u^{\mathrm{i}} = Au^{\mathrm{s}}(x,y), \tag{5.2}$$

where u^{s} is defined in (2.3). Thus the incident surface wave propagates in the positive x-direction. Let us assume for simplicity that the surface waves are pure surface waves, i.e. the impedance Z is given by (2.5). The angle $\theta_{\mathrm{c}} \in (0,\pi)$ describes the orientation of the screen with respect to the surface (see figure 6). The boundary conditions on the faces of the screen are

$$\partial u/\partial n = 0, \tag{5.3}$$

where n is the normal direction to the screen. The total field for the full-space problem can be written explicitly in terms of Fresnel functions. Far away from the tip, the total field may be written in the approximate form

$$u \sim u^{\mathrm{o}} + u^{\mathrm{d}}, \tag{5.4}$$

where u^{o} is the 'geometrical optics' field and u^{d} the field determined by the geometrical theory of diffraction. The geometrical optics field is illustrated in figure 6. The lines L_S and L_R represent the shadow and reflexion boundaries respectively. For zero impedance, i.e. $Y = \phi = 0$ (see (2.6)), they are the equivalent boundaries B_S and B_R for the incident body wave propagating in the positive x-direction. For $Y > 0$, they are displaced from the body wave boundaries towards the screen by an angle θ_Y, where

$$\sec\theta_Y = \cos\phi. \tag{5.5}$$

In the shadow zone $u^{\mathrm{o}} = 0$, while in the reflexion zone, $u^{\mathrm{o}} = u^{\mathrm{i}} + u^{\mathrm{r}}$, where the 'reflected' field u^{r} is

$$u^{\mathrm{r}} = u^{\mathrm{i}}(0,\bar{y})\exp[-\mathrm{i}kr\sin(\theta + 2\theta_{\mathrm{c}} - \phi)]. \tag{5.6}$$

This expression is equivalent to a surface wave below a surface at $\theta = \frac{3}{2}\pi - 2\theta_{\mathrm{c}}$, i.e. propagating along B_R in the direction away from the tip, with an amplitude of $u^{\mathrm{i}}(0,\bar{y})$ on this imaginary surface. It may happen that $\theta_Y > \theta_{\mathrm{c}}$, in which case the lines L_S and L_R of figure 6 are on the incident and 'shadow' sides of the tip respectively. In this case there is no reflexion zone. However, $u^{\mathrm{o}} = 0$ in the region between the screen and L_S, implying a 'shadow' zone on the illuminated side of the screen. We note that $\theta_{\mathrm{c}} < \frac{1}{2}\pi$ is a necessary condition for this peculiar event.

The diffracted field u^{d} of (5.4) is formally the same as that for a homogeneous plane wave incident upon the screen. The only difference is that the angle of incidence is now complex. We have

$$u^{\mathrm{d}} = u^{\mathrm{i}}(0,\bar{y})\,(kr)^{-\frac{1}{2}}\,\mathrm{e}^{\mathrm{i}kr}\,D(\theta+\tfrac{1}{2}\pi+\theta_{\mathrm{c}};\,\theta_{\mathrm{c}}-\phi), \tag{5.7}$$

where $D(\;;\;)$ is the usual acoustic diffraction coefficient:

$$D(\theta;\,\theta_0) = (2/\pi)^{\frac{1}{2}}\,\mathrm{e}^{\frac{1}{4}\mathrm{i}\pi}(\cos\theta-\cos\theta_0)^{-1}\cos\tfrac{1}{2}\theta\sin\tfrac{1}{2}\theta_0. \tag{5.8}$$

For homogeneous incidence, the relation (5.4) is not a uniformly asymptotic approximation. If the incident wave is evanescent, i.e. $Y > 0$, then the term u^{o} is exponentially smaller than u^{d}. In this case, (5.4) becomes a uniformly valid approximation. The correct form is

$$u = (u^{\mathrm{o}}+u^{\mathrm{d}})\,[1+O(1/kr)] = u^{\mathrm{d}}[1+O(1/kr)], \tag{5.9}$$

as $kr \rightarrow \infty$. Therefore the radiation function $E(\theta)$ of (4.5) may be expressed as

$$E(\theta) = u^{\mathrm{i}}(0,\bar{y})\,D(\theta+\tfrac{1}{2}\pi+\theta_{\mathrm{c}};\,\theta_{\mathrm{c}}-\phi) \equiv (8\pi)^{-\frac{1}{2}}\,\mathrm{e}^{\frac{1}{4}\mathrm{i}\pi}u^{\mathrm{i}}(0,\bar{y})f(\theta). \tag{5.10}$$

The fact that $D(\theta;\,\theta_0)$ blows up at $\theta = \theta_0$ implies that $E(\theta)$ is not analytic at the complex angles $\theta = 2n\pi-\frac{1}{2}\pi-\phi$, $2n\pi+\phi-\frac{1}{2}\pi-2\theta_{\mathrm{c}}$, where $n = 0, \pm 1, \pm 2, \ldots$. For homogeneous plane wave incidence, the singularities correspond to the shadow and reflexion boundaries, respectively.

Substituting the expression (5.10) for $E(\theta)$ in (4.18) and putting $E_{\mathrm{sc}} = 0$, we obtain for the magnitude of the scattered surface wave in the $\pm x$-direction the quantities

$$u^{\mathrm{i}}(0,\bar{y})f[\pm(\phi-\tfrac{1}{2}\pi)], \tag{5.11}$$

where $f(\theta)$ was defined in (5.10). Let us examine the forward- and back-scattered surface waves separately.

Forward-scattered surface wave

We have

$$f(\phi-\tfrac{1}{2}\pi) = \operatorname{cosec}\theta_{\mathrm{c}}-\operatorname{cosec}\phi. \tag{5.12}$$

Thus the magnitude of the forward-scattered surface wave blows up if either $\phi \rightarrow 0$ or $\theta_{\mathrm{c}} \rightarrow 0$ or π. The singularity at $\phi = 0$ corresponds to the shadow boundary for homogeneous incidence. When $\theta_{\mathrm{c}} \rightarrow 0$ or π, the singularity of $f(\phi-\frac{1}{2}\pi)$ is attributable to the reflexion boundary of evanescent waves. All of these singularities stem from the fact that the function $E(\theta)$ is not analytic for a semi-finite screen. For a screen of finite length, $E(\theta)$ is analytic, although it cannot be expressed in closed form. See Williams (1982) for a full discussion of the emission function in this case. Finally, we note from (5.11) that $f(\phi-\frac{1}{2}\pi)$, as a function of θ_{c}, is symmetric about $\theta_{\mathrm{c}} = \frac{1}{2}\pi$, at which angle its magnitude is a minimum.

Back-scattered surface wave

By definition of $f(\theta)$ we have

$$f(\tfrac{1}{2}\pi-\phi) = \sec(\theta_{\mathrm{c}}-\phi)-1, \tag{5.13}$$

and $$|f(\tfrac{1}{2}\pi-\phi)| = (\cosh|\phi| - \cos\theta_c)/(\cos^2\theta_c + \sinh^2|\phi|)^{\frac{1}{2}}. \tag{5.14}$$

The quantity $f(\frac{1}{2}\pi-\phi)$ blows up only if $\theta_c \to \frac{1}{2}\pi$ and simultaneously $|\phi| \to 0$; otherwise it remains bounded. This singularity corresponds to the shadow boundary for homogeneous incidence on a screen perpendicular to the free surface.

The graph of $|f(\frac{1}{2}\pi-\phi)|$ as a function of $\theta_c \in (0,\pi)$ is monotone increasing if

$$\cosh|\phi| > g^2 \quad (Y > g) \tag{5.15}$$

where $$g^2 = \tfrac{1}{2}(1+\sqrt{5}). \tag{5.16}$$

Otherwise, there is a maximum located at $\theta_c = \theta_{c,\max}$ where

$$\cos\theta_{c,\max} = -\sinh|\phi| \tanh|\phi|. \tag{5.17}$$

Thus, $\frac{1}{2}\pi < \theta_{c,\max} < \pi$, and

$$f(\tfrac{1}{2}\pi-\phi)|_{\theta_c=\theta_{c,\max}} = (1+\coth^2|\phi|)^{\frac{1}{2}}. \tag{5.18}$$

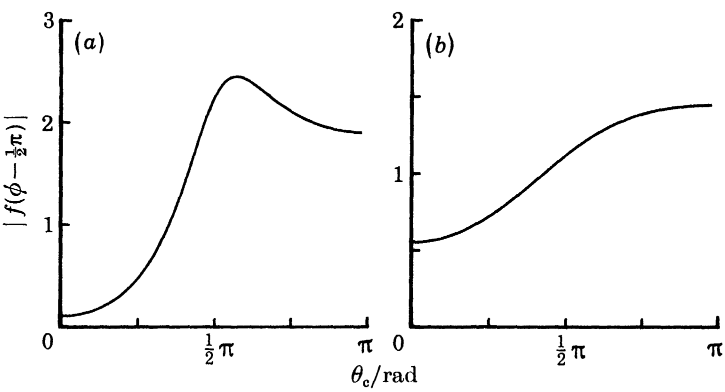

FIGURE 7. Magnitude of back-scattered surface wave from sub-surface screen for (*a*) $Y = 0.5$ and (*b*) $Y = 2.0$.

Therefore, if the impedance is small, i.e. $Y < g$, there exists an angle of inclination $\theta_c = \theta_{c,\max} \in (0,\pi)$, such that the back-scattered surface wave is maximized. The dependence of the back-scattered magnitude upon the inclination θ_c is illustrated in figure 7.

It is of interest to note that the results of this section give the surface waves generated by the diffraction of incident Love waves by the tip of a sub-surface crack. For this application $u(x,y)$ is identified as the displacement in the z-direction in an elastic solid.

This work was carried out in the course of research sponsored by the U.S. Army Research Office under grant DAAG29-80-C-0086 to Northwestern University.

References

Deschamps, G. A., Lee, S. W., Gowan, E. & Fontana, T. 1979 *Wave Motion* **1**, 25–35.
Gregory, R. D. 1970 *Proc. Camb. phil. Soc.* **67**, 689–710.
Jones, D. S. 1979 *Methods in electromagnetic wave propagation*. Oxford: Clarendon Press.
Keller, J. B. & Karal, F. C. 1960 *J. appl. Phys.* **31**, 1039–1046.
Morse, P. M. & Feshbach, H. 1953 *Methods of theoretical physics*. New York: McGraw-Hill.
Thiruvenkatachar, V. R. & Viswanathan, K. 1965 *Proc. R. Soc. Lond.* A **287**, 549–567.
Williams, M. H. 1982 *Q. Jl Mech. appl. Math.* **35**, 103–124.